Title: Cortical Processing of Arithmetic and Simple Sentences in an Auditory Attention Task

Abbreviated Title: Cortical Tracking of Spoken Equations & Sentences

Authors: Joshua P. Kulasingham[1], Neha H. Joshi[1,2]*, Mohsen Rezaeizadeh[1,2]* & Jonathan Z. Simon[1,2,3]

[1]Department of Electrical and Computer Engineering, [2]Institute for Systems Research,

[3]Department of Biology, University of Maryland, College Park, Maryland

*These authors contributed equally

Corresponding Author: Joshua P. Kulasingham, joshuapk@umd.edu

Conflict of Interest Statement: The authors declare no competing financial interests

Acknowledgements: This work was supported by DARPA (N660011824024), the National Science Foundation (SMA-1734892 and DGE-1449815), and the National Institutes of Health (R01-DC014085). The views, opinions and/or findings expressed are those of the authors and should not be interpreted as representing the official views or policies of the Department of Defense or the U.S. Government.

Abstract

Cortical processing of arithmetic and of language rely on both shared and task-specific neural mechanisms, which should also be dissociable from the particular sensory modality used to probe them. Here, spoken arithmetical and non-mathematical statements were employed to investigate neural processing of arithmetic, compared to general language processing, in an attention-modulated cocktail party paradigm. Magnetoencephalography data was recorded from 22 subjects listening to both sentences and arithmetic equations while selectively attending to one of the two speech streams. Short sentences and simple equations were presented diotically at fixed and distinct word/symbol and sentence/equation rates. Critically, this allowed neural responses to acoustics, words, and symbols to be dissociated from responses to sentences and equations. Indeed, the simultaneous neural processing of the acoustics of words and symbols was observed in auditory cortex for both streams. Neural tracking of sentences and equations, however, was predominantly of the attended stream, and originated primarily from left temporal, and parietal areas, respectively. Additionally, these neural responses were correlated with behavioral performance in a deviant detection task. Source-localized Temporal Response Functions revealed cortical dynamics of distinct responses to sentences in left temporal areas and equations in bilateral temporal, parietal and motor areas. Finally, the target of attention could be decoded from responses, especially in left superior parietal areas. In short, the neural responses to arithmetic and language are especially well segregated during the cocktail party paradigm, and the correlation with behavior suggests that these neural responses are linked to successful comprehension or calculation.

Significance Statement

Neural processing of arithmetic relies on dedicated, modality independent cortical networks that are distinct from those underlying language processing. Using a simultaneous cocktail party listening paradigm, we found that these separate networks segregate naturally when listeners selectively attend to one type over the other. Time-locked activity in the left temporal lobe was observed for responses to both spoken sentences and equations, but the latter additionally showed bilateral parietal activity consistent with arithmetic processing. Critically, these responses were modulated by selective attention and correlated with task behavior, consistent with reflecting high-level processing for speech comprehension or correct calculations. The response dynamics show task-related differences that were used to reliably decode the attentional target of sentences or equations.

1. Introduction

Comprehension and manipulation of numbers and words are key aspects of human cognition and share many common features. Numerical operations may rely on language for precise calculations (Spelke and Tsivkin, 2001; Pica et al., 2004) or share logical and syntactic rules with language (Houdé and Tzourio-Mazoyer, 2003). The cortical mechanisms underlying numerical and language processing have been widely studied. During numerical tasks, the frontal, parietal, occipital and temporal areas are activated (Menon et al., 2000; Dehaene et al., 2003, 2004; Arsalidou and Taylor, 2011; Maruyama et al., 2012; Dastjerdi et al., 2013; Harvey et al., 2013; Harvey and Dumoulin, 2017). Bilateral intraparietal sulcus (IPS) is activated by presenting numbers using Arabic or alphabetical notation (Pinel et al., 2001) or speech (Eger et al., 2003). Posterior parietal and prefrontal areas are activated for both arithmetic and language (Price, 2000;

Göbel et al., 2001; Venkatraman et al., 2006; Zarnhofer et al., 2012; Bemis and Pylkkänen, 2013). However, some cortical networks activated by numerical stimuli (e.g., intraparietal sulcus (IPS)), differ from those underlying language processing, even when the stimuli are presented using words (Amalric and Dehaene, 2016, 2019; Monti et al., 2012; Park et al., 2011). Lesion studies (Dehaene and Cohen, 1997; Varley et al., 2005; Baldo and Dronkers, 2007), further provide evidence that the neural basis of numerical processing is distinct from that of language processing (Gelman and Butterworth, 2005; Amalric and Dehaene, 2018).

The dynamics of these neural processes, beyond their cortical location, have also been investigated, and evoked responses to arithmetic processing have been found in parietal, occipital, temporal and frontal regions (Iguchi and Hashimoto, 2000; Kou and Iwaki, 2007; Ku et al., 2010; Jasinski and Coch, 2012; Maruyama et al., 2012; Iijima and Nishitani, 2017). Arithmetic operations have even been decoded from evoked responses (Pinheiro-Chagas et al., 2019). Speech studies have found early evoked components reflecting acoustic processing in auditory cortex, and later components reflecting linguistic and semantic processing in broader temporal, parietal and frontal regions (Baggio and Hagoort, 2011; Koelsch et al., 2004; Lau et al., 2008; Obleser et al., 2003, 2004). Linear models called Temporal Response Functions (TRFs) have been used to investigate time-locked responses to non-repetitive continuous speech (Lalor and Foxe, 2010), revealing dynamical processing of linguistic features (Brodbeck et al., 2018a, 2018b; Broderick et al., 2018; Di Liberto et al., 2015).

We utilize a technique pioneered by Ding et al. (2016) of presenting isochronous words and sentences (i.e., at fixed rates), to investigate higher order cortical processing of spoken language

and arithmetic. The single syllable word rate, also the dominant acoustic rate, is tracked strongly by auditory neural responses, as expected. However, cortical responses also strongly track the sentence rate, completely absent in the acoustics, which reflects hierarchical language processing (Sheng et al., 2018; Jin et al., 2020; Luo and Ding, 2020). When subjects selectively attend to one speech stream among several, in a 'cocktail party paradigm', the sentence rate is tracked only for the attended speaker (Ding et al., 2018). Similarly, cocktail party studies using TRFs show early auditory responses irrespective of attention, while responses to higher order speech features are modulated by attention (Ding and Simon, 2012; Brodbeck et al., 2018b). Attention modulates activation related to numerical processing as well (Castaldi et al., 2019).

Here, magnetoencephalography (MEG) is used to study the cortical dynamics of arithmetic and language processing of short sentences and simple arithmetic equations, presented at fixed word, symbol, sentence, and equation rates. We find evidence of neural tracking of equations in areas separately associated with language processing (e.g., temporal lobe, angular gyrus) and arithmetic processing (IPS, occipital lobe), and demonstrate that these cortical networks segregate naturally during selective attention. Neural tracking of equations and sentences is correlated with behavioral performance, suggesting that these responses may be linked to comprehension and/or arithmetic computations.

2. Methods

2.1. Participants

MEG data was collected from 22 adults (average age 22.6 yrs, 10 female, 21 right handed) who were native English speakers. The participants gave informed consent and received monetary compensation. All experimental procedures were approved by the Internal Review Board of the University of Maryland, College Park. To ensure that the subjects could satisfactorily perform the arithmetic task, only subjects who self-reported that they had taken at least one college level math course were recruited.

2.2. Speech stimuli

Monosyllabic words were synthesized with both male and female speakers using the ReadSpeaker synthesizer (https://www.readspeaker.com, 'James' and 'Kate' voices). The language stimuli consisted of 4-word sentences and the arithmetic stimuli consisted of 5-word equations (hereafter, arithmetic words are referred to as 'symbols', arithmetic sentences as 'equations', non-arithmetic words as 'words' and non-arithmetic sentences as 'sentences'). The words and symbols were modified to be of constant durations to allow for separate word, symbol, sentence and equation rates, so that the neural response to each of these could be separated in the frequency domain. The words and symbols were constructed with fixed durations of 375 ms and 360 ms respectively, giving a word rate of 2.67 Hz, a symbol rate of 2.78 Hz, a sentence rate of 0.67 Hz, and an equation rate of 0.55 Hz. All the words and symbols were mono-syllabic, and hence the syllabic rate is identical to the word/symbol rate. These rates are quite fast for spoken English, and, though intelligible, can be difficult to follow in the cocktail party conditions. Because neural signals below 0.5 Hz are very noisy, however, it was not deemed appropriate to reduce the rates further;

preliminary testing showed that these rates were a suitable compromise between ease of understanding and reasonable neural signal to noise ratio. In addition, the rates were selected such that 10 equations and 12 sentences (each of which make up a single "trial") would have the same duration, allowing for precise frequency resolution at both these rates.

The individual words and symbols were shortened by removing silent portions before their beginning and after their end, and then manipulated to give durations of 375 ms and 360 ms respectively, using the overlap-add resynthesis method in Praat (Boersma and Weenick, 2018). The words and symbols were respectively formed into sentences and equations (described below) and were lowpass filtered below 4 kHz using a 3rd order elliptic filter (the air-tube system used to deliver the stimulus has a lowpass transfer function with cutoff approximately 4 kHz). Finally, each stimulus was normalized to have approximately equal perceptual loudness using the MATLAB 'integratedLoudness' function. Although this succeeded in giving all stimuli similar perceptual loudness, it also resulted in the acoustic spectra showing a stronger word rate peak than the symbol rate peak (see Fig. 1B). This byproduct, however, was not observed to carry over in the neural response spectrum.

The equations were constructed using a limited set of symbols consisting of the word 'is' (denoting '='), three operators ('plus' (+), 'less' (-) and 'times' (×)), and the eleven English monosyllabic numbers ('nil', 'one' through 'six', 'eight' through 'ten', and 'twelve'). The equations themselves consisted of a pair of monosyllabic operands (numbers) joined by an operator, an 'is' statement of equivalence, and a monosyllabic result; the result could be either the first or last symbol in the equation (e.g., 'three plus two is five' or 'five is three plus two'). The equations were randomly

generated with repetitions allowed, in order to roughly balance the occurrences of each number (although smaller numbers are still more frequent since there are more mathematically correct equations using only the smallest numbers). The fact that the symbol 'is' occurs in every sentence, in either the 2nd or 4th position, is an additional regularity, which led to additional peaks in the acoustic stimulus spectrum at the first and second harmonic of the equation rate (1.11 Hz and 1.66 Hz) as seen in Fig. 1. Although less than ideal, it is difficult to avoid in a paradigm when restricting to mathematically well-formed equations. Hence, we do not analyze the neural responses at those harmonic frequencies, since their relative contributions from auditory vs. arithmetic processing are not simple to estimate. The sentences were also constructed with two related syntactic structures to be similar to the two equation formats: verb in second position (e.g., 'cats drink warm milk') and verb in third position (e.g., 'head chef bakes pie'), but unlike the 'is' of the arithmetic case, the verb changed with every sentence and there were no analogous harmonic peaks in the sentence case. Deviants were also constructed: deviant equations were properly structured but mathematically incorrect (e.g., 'one plus one is ten'); analogously, deviant sentences were syntactically correct but semantically nonsensical (e.g., 'big boats eat cake'). Cocktail party stimuli were constructed by adding the acoustic waveforms of the sentences and equations in a single audio channel (see Fig. 1) and presented diotically (identical for both ears). The speakers were different (male and female), in order to simplify the task of segregating diotically presented speech. The mixed speech was then normalized to have the same loudness as all the single speaker stimuli using the abovementioned algorithm.

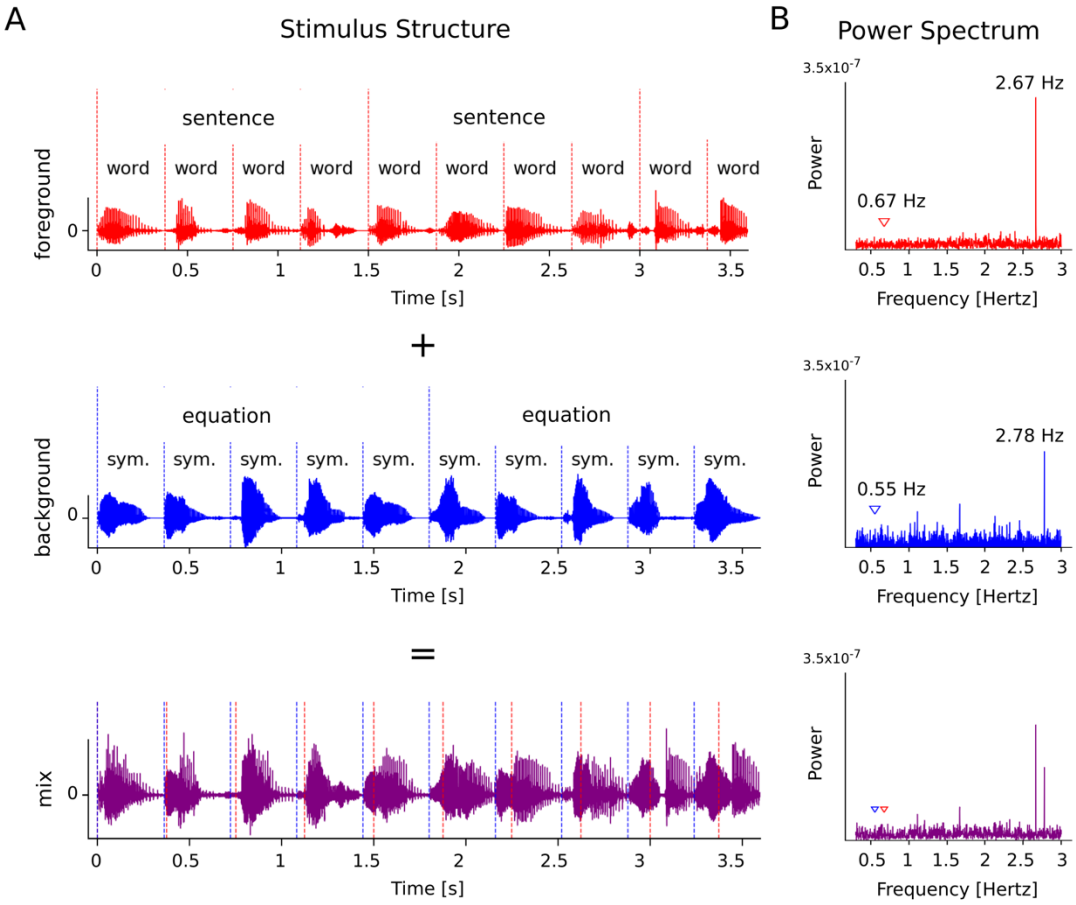

Figure 1: Stimulus structure. A. The foreground, background and mix waveforms for the initial section of the stimulus for a two-speaker attend-language trial. The sentence, equation, word and symbol structures are shown. The word and symbol rhythms are clearly visible in the waveforms. The mix was presented diotically and is the linear sum of both streams. **B.** The frequency spectrum of the entire stimulus. Clear word and symbol rate peaks are seen in the foreground and background respectively, while the mix spectrum has both peaks. The sentence rate (0.67 Hz) and equation rate (0.55 Hz) are denoted by the red and blue triangles respectively. Note that there are no sentence rate or equation rate peaks in the stimulus spectrum.

2.3. Experimental design

The experiment was conducted in blocks: 4 single speaker blocks (2 × 2: male and female, sentences and equations) were followed by 8 cocktail party blocks (a new example of each of the

above stimuli mixed with a new example of the opposite stimulus type, presented twice). The blocks alternated between attending to math or language, and male or female speakers. Each block consisted of multiple trials (10 for single speaker, 6 for cocktail party). 50% of the blocks had one outlier trial. Each trial was 18 s in duration and consisted of 10 equations or 12 sentences (or both, for cocktail party conditions). In total, the single speaker conditions had 240 sentences and 200 equations, and the cocktail party conditions had 288 sentences and 240 equations in the foreground. Deviant trials had one equation/sentence being a deviant. At the start of each block, the subject was instructed which stimulus to attend to, and to press a button at the end of each trial to indicate whether a deviant was detected (right button: yes, left button: no). The subjects kept their eyes open and a screen indicated which voice they should attend to ('Attend Male' or 'Attend Female') while the stimulus was presented diotically. After each trial, the stimulus was paused, and the screen displayed the text 'Outlier?' until the subjects pressed one of the two buttons. There was a 2 second break after the button press, after which the next trial stimulus was presented.

Since the deviant detection task was challenging, especially in the cocktail party case, subjects were asked to practice detecting deviants just before they were placed inside the MEG scanner (2 trials of language, 2 trials of arithmetic with stimuli not used during the experiment). The majority of subjects reported that it was easier to follow and detect deviants in the equations compared to the sentences. This might arise for several reasons, e.g., because the equations had a restricted set of simple numbers, or because the repetitive 'is' symbol helped keep track of equation structure.

2.4. MEG data acquisition and preprocessing

A 157 axial gradiometer whole head MEG system (Kanazawa Institute of Technology, Nonoichi, Ishikawa, Japan) was used to record MEG data while subjects rested in the supine position in a magnetically shielded room (VAC, Hanau, Germany). The data was recorded at a sampling rate of 2000 kHz with an online 200 Hz low pass filter, and a 60 Hz notch filter. Saturating channels were excluded (approximately two channels on average) and the data was denoised using time-shift principal component analysis (de Cheveigné and Simon, 2007) to remove external noise, and sensor noise suppression (de Cheveigné and Simon, 2008) to suppress channel artifacts. All subsequent analyses were performed in mne-python 0.19.2 (Gramfort, 2013; Gramfort et al., 2014) and eelbrain 0.33 (Brodbeck et al., 2020). The MEG data was filtered from 0.3–40 Hz using a delay compensated FIR filter (mne-python 0.19.2 default settings), downsampled to 200 Hz, and independent component analysis was used to remove artifacts such as eye blinks, heartbeats and muscle movements.

2.5. Frequency domain analysis

The complex-valued spectrum of the MEG response for each sensor was computed using the Discrete Fourier Transform (DFT). The preprocessed MEG responses were separated into 4 conditions: attending math or language, in single speaker or cocktail party conditions. The male and female speaker blocks were combined for all analysis. Within each condition, the MEG responses for each trial were concatenated to form signals of duration 6 minutes for each of the single speaker conditions and 7.2 minutes for each of the cocktail party conditions. The DFT was computed for each sensor in this concatenated response, leading to a frequency resolution of 2.7×10^{-3} Hz for the single speaker conditions and 2.3×10^{-3} Hz for the cocktail party conditions.

The amplitudes of the frequency spectra were averaged over sensors and tested for significant frequency peaks (described in section 2.9).

Frequencies of interest were selected corresponding to the equation rate (0.555 Hz), the sentence rate (0.667 Hz), the symbol rate (2.778 Hz), and the word rate (2.667 Hz). Note that the duration of the signals is an exact multiple of both the symbol and the word durations, ensuring that the frequency spectrum contained an exact DFT value at each of these four rates. In addition, the neighboring 5 frequency values on either side of these key frequencies were also selected to be used in a noise model for statistical tests.

2.6. Neural source localization

The head shape of each subject was digitized using a Polhemus 3SPACE FASTRAK system, and head position was measured before and after the experiment using five marker coils. The marker coil locations and the digitized head shape were used to co-register the template FreeSurfer 'fsaverage' brain (Fischl, 2012) using rotation, translation and uniform scaling. A volume source space was formed by dividing the brain volume into a grid of 12 mm sized voxels. This source space was used to compute an inverse operator using minimum norm estimation (MNE) (Hämäläinen and Ilmoniemi, 1994), with a noise covariance estimated from empty room data. The complex-valued sensor distributions of each of the 44 selected frequencies (4 frequencies of interest with 10 sidebands each) were localized independently using MNE onto the volume source space, forming complex-valued source activations. The amplitudes of these complex-valued source activations were used for subsequent analysis. The sideband source distributions were averaged together to form the noise model.

2.7. Temporal Response Functions (TRFs)

The preprocessed MEG responses in each of the four conditions were source-localized in the time domain using MNE, similar to the method described above in the frequency domain. The MEG signals were further lowpassed below 10 Hz using a delay compensated FIR filter (default settings in mne python) and downsampled to 100 Hz for the TRF analysis. These responses were then used along with representations of the stimulus to estimate TRFs. The linear TRF model for P predictors (stimulus representations) is given by

$$y(t) = \sum_{p=1}^{P} \sum_{d} \tau^{(p)}(d)\, x^{(p)}(t-d) \; + n(t) \tag{1}$$

where $y(t)$ is the response at a neural source at time t, $x^{(p)}(t-d)$ is the time shifted p^{th} predictor (e.g., speech envelope, word onsets, etc., as explained below) with time lag of d, $\tau^{(p)}(d)$ is the value of the TRF corresponding to the pth predictor at lag d, and $n(t)$ is the residual noise. The TRF estimates the impulse response of the neural system for that predictor, and can be interpreted as the average time-locked response to continuous stimuli (Lalor and Foxe, 2010). For this analysis, several predictors were used to estimate TRFs at each neural source using the boosting algorithm (David et al., 2007), as implemented in eelbrain, thereby separating the neural response to different features. The boosting algorithm may result in overly sparse TRFs, and hence an overlapping basis of 30 ms Hamming windows (with 10 ms spacing) was used in order to allow smoothly varying responses. For the volume source space, the TRF at each voxel for a particular predictor is a vector that varies over the time lags, representing the amplitude and direction of the current dipole activity.

The stimulus was transformed into 2 types of representations that were used for TRF analysis: acoustic envelopes and rhythmic word/symbol or sentence/equation onsets. Although we were primarily interested in responses to sentences and equations, a linear model with only sentence/equation onsets would be disadvantaged by the fact that these representations are highly correlated with the acoustics. Hence by jointly estimating the acoustic envelope and word onset TRFs in the model, the lower level acoustic responses are automatically separated, allowing the dominantly higher-level processing to emerge in the sentence/equation TRFs. The acoustic envelope was constructed using the 1-40 Hz bandpassed Hilbert envelope of the audio signal (delay compensated FIR filter used above). The onset representations were formed by placing impulses at the regular intervals corresponding to the onset of the corresponding linguistic unit. The four onset responses were: impulses at 375 ms spacing for word onsets, 360 ms for symbol onsets, 1500 ms for sentence onsets, and 1800 ms for equation onsets. Values at all other time points in these onset representations were set to zero. In order to separate out responses to stimulus onset and offset, the first and last sentences were assigned separate onset predictors, which were not analyzed further except to note that their TRFs showed strong and sustained onset and offset response, respectively, unlike the remaining sentence TRFs. The remaining (middle) sentences' onsets were combined into one predictor that was used for further analysis. The same procedure was followed for the equation onset predictors.

For each of the two single-speaker conditions, 5 predictors were used in the TRF model: the corresponding sentence/equation onsets (just described), word/symbol onsets and the acoustic envelope. For each of the two cocktail conditions, 10 predictors were used in the TRF model: the abovementioned 5 predictors, for each of the foreground and the background stimuli. The

predictors were fit in the TRF model jointly, without any preference given to one of them over another.

The TRF for the speech envelope and the word/symbol onsets were estimated for time lags of 0-350 ms in order to limit the TRF duration to before the onset of the next word (at 375 ms) or symbol (at 360 ms). The sentence and equation TRFs were estimated starting from 350 ms to avoid onset responses, as well as lagged responses to the previous sentence. The sentence TRF was estimated until 1850 ms (350 ms past the end of the sentence) and the equation TRF was estimated until 2150 ms (350 ms past the end of the equation), in order to detect lagged responses. These sentence and equation TRFs were used to further analyze high level arithmetic and language processing.

2.8. Decoder analysis

All decoding analyses were performed using scikit-learn (Pedregosa et al., 2011) and mne-python software. To investigate the temporal dynamics of responses, linear classifiers were trained on the MEG sensor space signals bandpassed 0.3-10 Hz at 200 Hz sampling frequency. Decoders were trained directly on the sensor space signals, since the linear transformation to source space cannot increase the information already present in the MEG sensor signals. The matrix of observations $\mathbf{X} \in \mathbb{R}^{N \times M}$, for N samples and M sensors in each sample, was used to predict the vector of labels $\mathbf{y} \in \{0, 1\}^N$ at each time point of sentences or equations. The labels correspond to the two attention conditions (attend math or attend language). The decoders were trained in the single speaker conditions on time points from 0 to 1500 ms for both sentences (duration 1500 ms) and equations

(duration 1800 ms). Therefore, the decoder at each time point learns to predict the attended stimulus type (math or language) using the MEG sensor topography at that time point.

In a similar manner, the operator type in the arithmetic condition was also decoded from the MEG sensor topographies at each time point, in the 720 ms time window of each equation that contained the operator and its subsequent operand. 3 decoders were trained for the 3 comparisons ('plus' vs. 'less', 'less' vs. 'times' and 'plus' vs. 'times').

To further investigate the patterns of cortical activity, linear classifiers were trained on the source localized MEG responses at each voxel, with $\mathbf{X} \in \mathbb{R}^{N \times T}$ for N samples and T time points in each sample. Two types of classifiers were used. 1) Decoding based on first words: The first symbol of each equation and first word of each sentence was used as the sample, with a label denoting attend math or attend language conditions. 2) Decoding based on last words: The last symbol or word was used. Words of duration 375 ms were downsampled to match the duration of the symbols (360 ms), in order to have equal length training samples. This method was used separately for both the single speaker and the cocktail party conditions. The decoder at each voxel learns to predict the attended stimulus type (math or language) using the temporal dynamics of the response at that voxel.

Finally, the effect of attention was investigated using two sets of classifiers for math and language at each voxel. For the attend-math classifier, the cocktail party trials were separated into samples at the equation boundaries (12 equations per trial), and the labels were marked as '1' when math was attended to and '0' when not. The time duration T was 0-1800 ms (entire equation). For the

attend-language classifier, the cocktail party trials were separated into samples at the sentence boundaries (10 sentences per trial) and the labels were '1' when attending to language and '0' otherwise. The time duration T was 0-1500 ms (entire sentence). Therefore, the attend-math decoder at each voxel learns to predict whether the math stimulus was attended to using the temporal dynamics of the response to the equation at that voxel (and similarly for the attend-language decoder).

In summary, the decoders at each time point reveal the dynamics of decoding attention to math vs. language from MEG sensor topographies, and the decoders at each voxel reveal the ability to decode arithmetic and language processing in specific cortical areas. The trained classifiers were tested on a separate set and the score of the decoder was computed. Logistic regression classifiers were used, with 5-fold cross-validation, within-subject for all the trials. The area under the receiver operating characteristic curve (*AUC*) was used to quantify the performance of the classifiers.

2.9. Statistical analysis

The power spectrum for each condition was averaged across sensors, and permutation tests were used to detect significant peaks across subjects. Each frequency value in the spectrum from 0.3 to 3 Hz was tested for a significant increase over the neighboring 5 values on either side using 10000 permutations and the max-t method (Nichols and Holmes, 2002) to adjust for multiple comparisons.

The source distributions for each individual were mapped onto the FreeSurfer 'fsaverage' brain, in order to facilitate group statistics. To account for individual variability and mislocalization

during this mapping, the distributions were spatially smoothed using a Gaussian window with a standard deviation of 12 mm for all statistical tests. The source localized frequency responses were tested for a significant increase over the noise model formed by averaging the corresponding 10 source localized sidebands. Nonparametric permutation tests (Nichols and Holmes, 2002) and Threshold Free Cluster Enhancement (TFCE) (Smith and Nichols, 2009) were performed to compare the response against the noise and to control for multiple comparisons. A detailed explanation of this method can be found in Brodbeck et al. (2018). Briefly, a test statistic (in this case, paired samples t-statistics between true responses and noise models) is computed for the true data and 10000 random permutations of the data labels. The TFCE algorithm is applied to these statistics, in order to enhance continuous clusters of large values and a distribution consisting of the maximum TFCE value for each permutation is formed. Any value in the original TFCE map that exceeds the 95th percentile is considered significant at the 5% significance level. In all subsequent results, the minimum p-value and the maximum or minimum t-value across voxels is reported as p_{min}, t_{max} or t_{min} respectively. Lateralization tests were performed by testing each voxel in the left hemisphere with the corresponding voxel in the right, using permutation tests and TFCE with paired samples t-statistics. For the attend math conditions, equations were separated by operator type ('plus' (+), 'less' (-) or 'times' (×)) to test for specific responses to each operator. No significant differences were found between the source localized responses to each operator.

Behavioral responses for the deviant detection task were classified as either correct or incorrect, and the number of correct responses for each subject was correlated with the source localized response power of that subject. The noise model for each frequency of interest was subtracted from the response power before correlating with behavior. Nonparametric permutation tests with TFCE

were used in a manner similar to that given above. The only difference was that the statistic used for comparison was the Pearson correlation coefficient between the two variables (behavior and response power), and not the t-statistic, and the maximum correlation coefficient across voxels is reported as r_{max}.

The TRFs were tested for significance using vector tests based on Hotelling's T^2 statistic (Mardia, 1975). Since the TRFs consist of time varying vectors, this method tests for consistent vector directions across all subjects at each time point and each voxel. The Hotelling's T^2 statistic was used with non-parametric permutation tests and TFCE as described above, with the added dimension of time, and the maximum T^2 statistic across voxels is reported as T^2_{max}. This statistic is more suitable than a t-statistic based on the amplitude of the TRF vectors, since activation from distinct neural processes may have overlapping localizations (due to the limited resolution of MEG), but different current directions. Similarly, for the cocktail party conditions, foreground and background TRFs were compared in order to assess attentional effects, using the difference vector of the two TRFs.

Finally, the decoders were tested across subjects for a significant increase in decoding ability above chance ($AUC = 0.5$) at each time point or at each voxel. Multiple comparisons were controlled for using permutation tests and TFCE, similar to the above cases, with AUC as the test statistic.

3. Results

3.1 Behavioral results

After each trial, subjects indicated whether that trial contained a deviant by pressing a button. The single speaker conditions had higher deviant detection accuracies (arithmetic: mean = 89.9%, std. = 10.7%; language: mean = 74%, std. = 13.7%) than the cocktail party conditions (arithmetic: mean = 79.8%, std. = 13.6%; language: mean = 62.3%, std = 18.9%). Subjects reported that the arithmetic was perceptually easier to follow than the sentences, consistent with the fact that the equations were formed using a smaller set of symbols (restricted to being monosyllabic numbers to preserve the symbol rates). The presence of 'is' in each equation may have also contributed to subjects tracking equation boundaries.

3.2. Frequency domain analysis

The response power spectrum was averaged over sensors and a permutation test with the max-t method was performed to check whether the power at each frequency of interest was significantly larger than the average of the neighboring 5 frequency bins on either side (see Fig. 2). For the language single speaker condition, the sentence rate (0.67 Hz, $t = 7.25$, $p < 0.001$), its first harmonic (1.33 Hz, $t = 6.11$, $p = 0.0023$), and the word rate (2.67 Hz, $t = 12.98$, $p < 0.001$) were significant (one tailed permutation test of difference of amplitudes with max-t method). Similarly, for the math single speaker condition, the symbol rate (2.78 Hz, $t = 12.39$, $p < 0.001$) and the equation rate (0.55 Hz, $t = 6.29$, $p = 0.0017$) were significant. In this condition, the 1st and 2nd harmonics of the equation rate were also significant ($t = 7.28$, $p < 0.001$ at 1.11Hz; $t = 7.77$, $p < 0.001$ at 1.67 Hz). Thus, in both conditions, the responses track the corresponding sentence or equation rhythms that are not explicitly present in the acoustic signal. The harmonic peak (1.33 Hz) in the language

condition are consistent with phrase tracking (Ding et al., 2016), and the harmonics in the arithmetic condition (1.11 Hz, 1.66 Hz) are consistent with acoustic properties of the stimulus due the required occurrence of an operator in one of two positions (see Methods 2.2), or higher-order processing, or both.

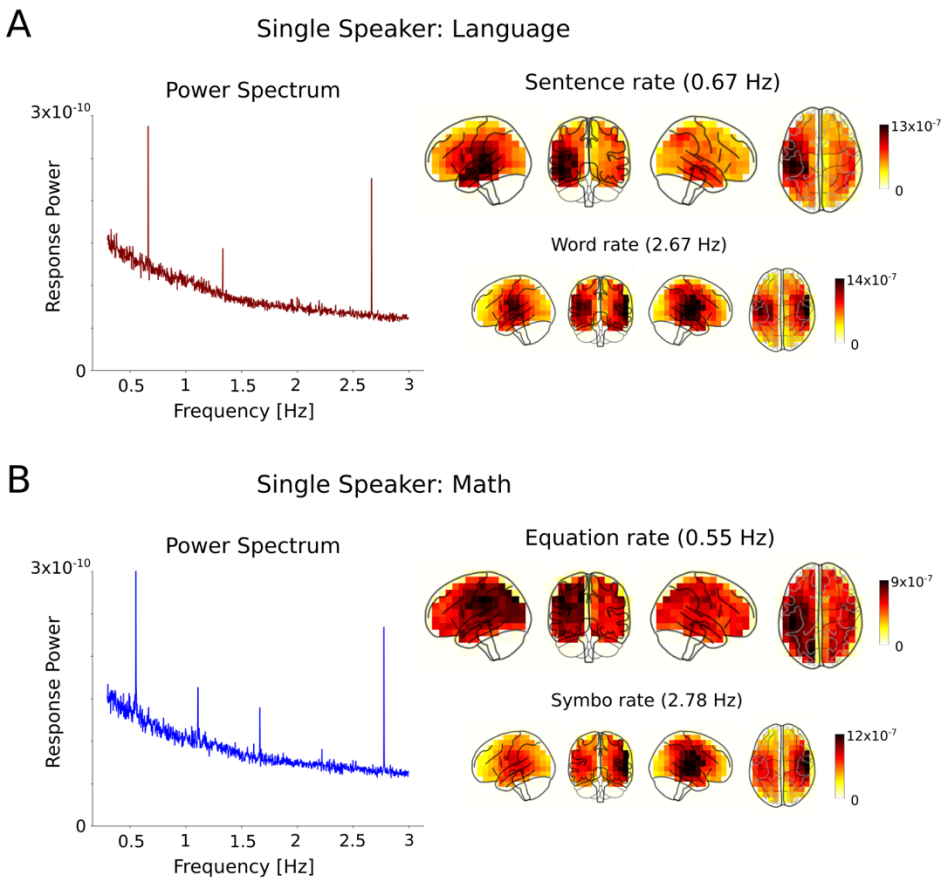

Figure 2. Response spectrum in the single speaker conditions. The MEG response as a function of frequency for the (A) language and (B) math conditions. The power spectrum, averaged over sensors and subjects, is shown on the left. Clear peaks are seen at the sentence, equation, word and symbol rates. The source localized response power at critical frequencies, averaged over subjects and masked by significant increase over the noise model, is shown on the right. Because the number of repetitions of sentences, equations, words and symbols is different,

and because the background neural activity changes at different frequencies, the amplitudes of each response peak are not directly comparable (color scales are normalized within each subplot in order to clearly show the spatial patterns). The word and symbol rate powers are maximal in bilateral auditory cortical areas, while the sentence rate power is maximal in left temporal lobe. The equation rate power shows a broad distribution, predominantly in left parietal and occipital areas.

For the attend-language cocktail party condition, only the (attended) word, (unattended) symbol and (attended) sentence rates were significant (one tailed permutation test of difference of amplitudes with max-t method; $t = 9.29$, $p < 0.001$; $t = 10.59$, $p < 0.001$; $t = 5.46$, $p = 0.0195$ respectively) as shown in Fig 3. The (unattended) equation rate was not significant. On the other hand, for the attend-arithmetic cocktail party condition, the (unattended) word, (attended) symbol and (attended) equation rates were significant ($t = 10.86$, $p < 0.001$; $t = 11.64$, $p < 0.001$; $t = 6.07$, $p = 0.005$ respectively), while the (unattended) sentence rate was not significant. The 1st and 2nd harmonics of the equation rate were also significant in attend math condition (1.11 Hz, $t = 5.31$, $p = 0.024$; 1.67 Hz, $t = 5.09$, $p = 0.04$). Since the word and symbol rates are present in the acoustics for both conditions, the neural responses at these rates could merely reflect acoustic processing. However, the fact that the sentence and equation rates are significant only in the corresponding attention condition suggests that these responses may dominantly reflect attention-selective high-level processes. This agrees with prior studies showing a similar effect for language (Ding et al., 2018). Here we show that this effect occurs even for arithmetic equations. However, arithmetic equations are also sentences, so it is unclear from this result alone if the equation peak reflects merely tracking of sentential structure and not arithmetic processing. To investigate this, we used volume source localization to determine the distribution of power over the cortex for these frequency peaks.

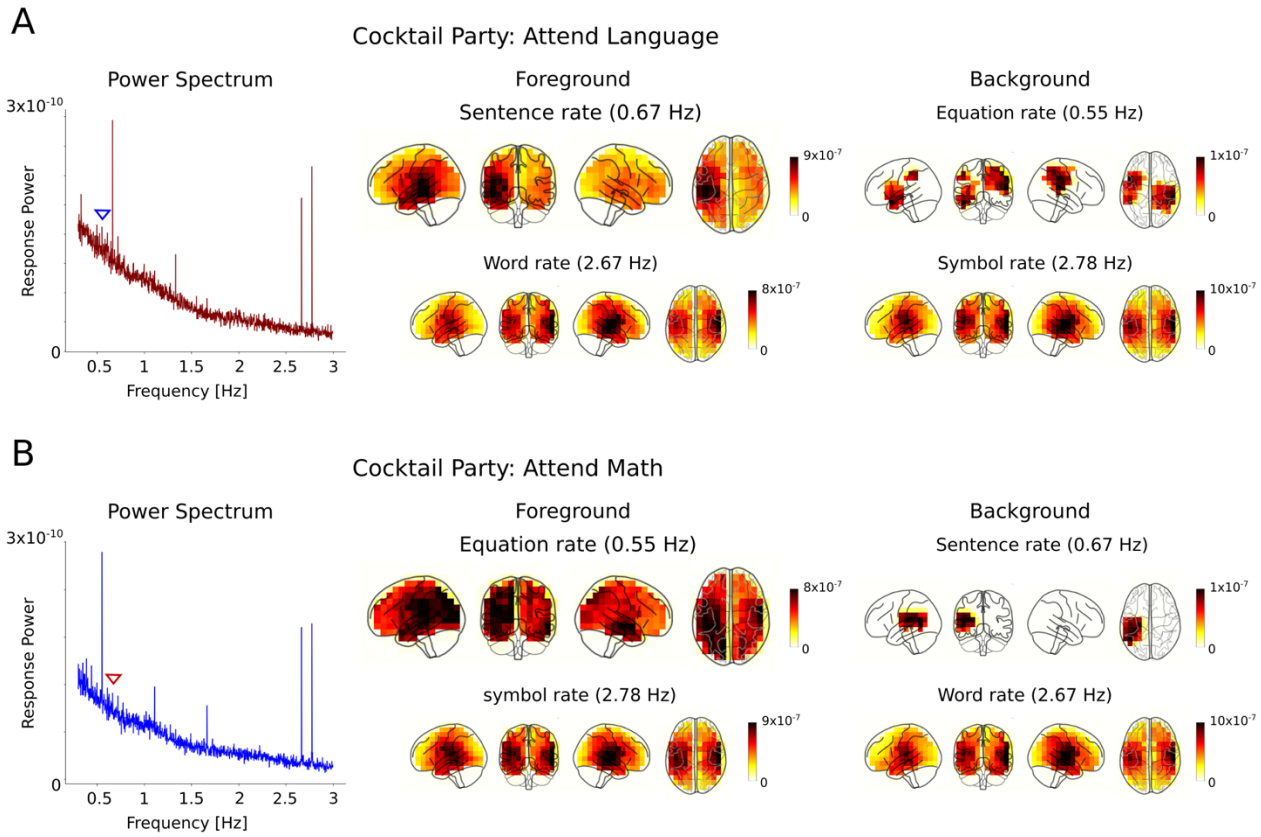

Figure 3. Response spectrum in the cocktail party conditions. The MEG response as a function of frequency for the (A) attend-language and (B) attend-math conditions. The power spectrum, averaged over sensors and subjects, is shown on the left. Clear double peaks are seen for word and symbol rates, irrespective of attentional focus. However, the sentence and equation rate peaks are only present during their corresponding attention condition. There are no analogous peaks at the background sentence and equation rates, indicated by the red and blue triangles respectively. The source localized response power is shown on the right as in Fig. 2., with color scales again normalized within each subplot. The localization of the response powers follows a similar pattern to that seen in Fig. 2 for word and symbol rates and for the foreground sentence and equation rate. Although the background sentence and equation rates show significant activity, the amplitude of these responses are much smaller than the responses at the corresponding attended rates.

The responses at the 4 frequencies of greatest interest (word, symbol, sentence and equation rates) were source-localized using the sensor topography of the complex-valued frequency spectrum. The amplitudes of the resulting complex-valued volume source distributions were used as an estimate of the neural power. For each frequency of interest, the neighboring 5 bins on either side were also source localized and averaged together to form an estimate of the background noise. The response power distribution for each of these frequencies were tested for a significant increase in power over the noise estimate using nonparametric permutation tests with paired sample t-statistics and TFCE. For both single speaker conditions, the corresponding word or symbol powers were significant (t_{max} = 12.85, p_{min} < 0.001, and t_{max} = 12.77, p_{min} < 0.001, respectively) in the regions shown in Fig. 2, with the average power being strongest in bilateral auditory cortex. The word and symbol rate responses were not significantly different (t_{min} = -2.11, t_{max} = 3.63, p > 0.08), consistent with low level auditory processing. The corresponding sentence or equation powers were also significant (t_{max} = 9.92, p_{min} < 0.001, and t_{max} = 7.68, p_{min} < 0.001, respectively). The source power distributions were visually quite different: for sentences, the response power was predominantly in left auditory cortex and temporal lobe, whereas for equations the response power was distributed over wide areas of bilateral temporal, parietal and occipital lobes. Despite these visually distinct patterns, the two responses were not significantly different (t_{min} = -3.00, t_{max} = 3.36, p > 0.12), perhaps because large portions of the brain show activity synchronized to the rhythm. Both sentence and equation responses were significantly left lateralized in temporal (t_{max} = 6.69, p_{min} < 0.001) and parietal (t_{max} = 3.9, p_{min} = 0.009) areas respectively. No significant differences were seen in the responses at the equation rate when separated according to operator type ('+' vs. '-': t_{min} = -2.98, t_{max} = 1.64, p > 0.34; '-' vs. '×': t_{min} = -2.08, t_{max} = 3.21, p > 0.39; '×' vs. '+': t_{min} = -2.26, t_{max} = 3.01, p > 0.31).

For the cocktail party conditions, similar results were obtained for both word and symbol rate responses (attend language word rate: $t_{max} = 11.9$, $p_{min} < 0.001$, attend math word rate: $t_{max} = 11.1$, $p_{min} < 0.001$, attend language symbol rate: $t_{max} = 12.8$, $p_{min} < 0.001$, attend math symbol rate: $t_{max} = 11.01$, $p_{min} < 0.001$). The power was predominantly from bilateral auditory cortices as shown in Fig. 3, and the symbol and word rates were not significantly different ($t_{min} = -4.31$, $t_{max} = 2.33$, $p > 0.16$). The attended sentence or equation rate responses were significant ($t_{max} = 6.78$, $p_{min} < 0.001$, and $t_{max} = 7.87$, $p_{min} < 0.001$, respectively) and the localization was similar to the single speaker case, albeit more bilateral for the equation rate response. Indeed, the sentence rate response was significantly left lateralized ($t_{max} = 5.36$, $p_{min} < 0.001$), similar to the single speaker case, but the equation rate response was not ($t_{max} = 2.97$, $p > 0.067$). However, the spatial distribution of the equation rate response was visually larger in the left hemisphere (see Fig. 3); indeed, the source localization of attended sentence power and attended equation power were significantly different ($t_{min} = -4.77$, $t_{max} = 2.39$, $p_{min} = 0.013$), with more equation rate power in the right hemisphere. This indicates that the equation rate power does not originate from the same cortical regions that give rise to the sentence rate response and that the selective attention task is better able to separate these responses. Surprisingly, the unattended sentence and equation rates were also significant ($t_{max} = 4.02$, $p_{min} = 0.005$, and $t_{max} = 5.31$, $p_{min} < 0.001$, respectively), though in a very small number of voxels, consistent with the idea that participants sometimes inadvertently switched attentional focus. The locations of these significant voxels (near auditory cortex for sentences, near IPS for equations) provide further evidence for the fact that these responses reflect differential neural processing of sentences and equations.

3.3. Behavioral correlations

The behavioral responses were correlated with source localized response power using non-parametric permutation tests with TFCE, using Pearson correlation as the test statistic. Deviant detection performance for sentences in the single speaker condition was significantly correlated with the neural power at the sentence rate (p_{min} = 0.02, maximum correlation in significant regions r_{max} = 0.62) as shown in Fig. 4. However, detection of equation deviants in the single speaker condition was not significantly correlated with the neural power at the equation rate; this may be related to the fact that performance in the single speaker arithmetic condition was at ceiling for several participants. The performance when detecting sentence deviants in the cocktail party conditions was correlated with the attended sentence rate power (r_{max} = 0.62, p_{min} = 0.015), attended word rate power (r_{max} = 0.64, p_{min} = 0.03) as well as the unattended symbol rate power (r_{max} = 0.79, p_{min} = 0.001). The performance when detecting equation deviants in the cocktail party condition was correlated with the attended equation rate power (r_{max} = 0.6, p_{min} = 0.02) and the unattended word rate power (r_{max} = 0.74, p_{min} = 0.04). It was unexpected that the unattended word and symbol rate powers were significantly correlated with behavior, and possible explanations are discussed in section 4.3. Critically, however, sentence and equation rate powers were correlated with behavior only when attended.

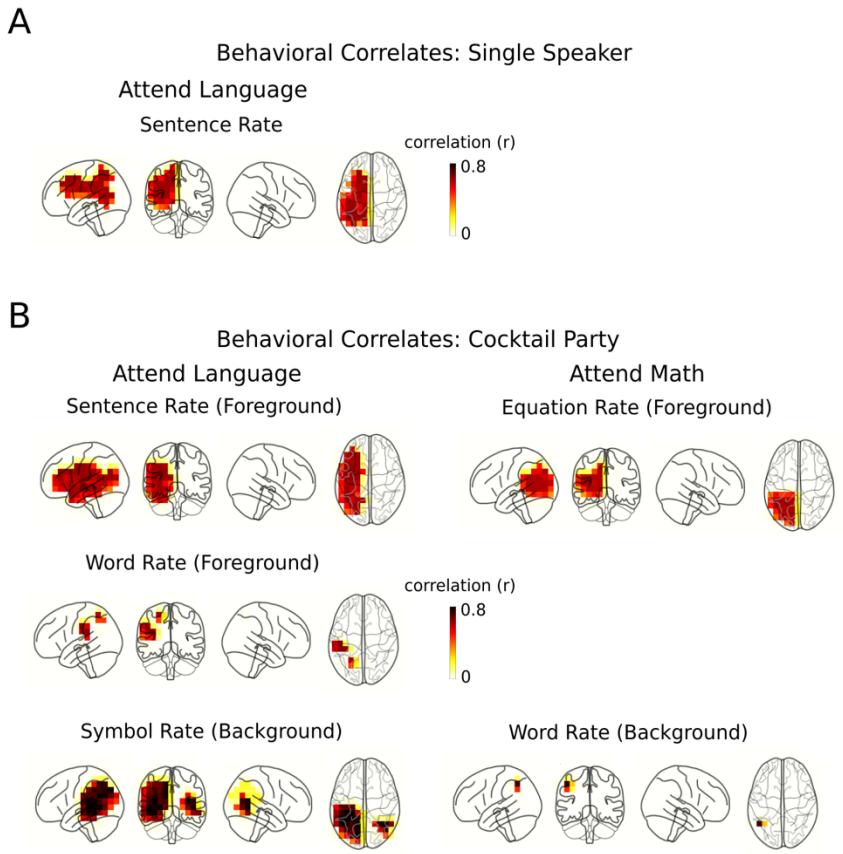

Figure 4. Response power correlations with behavior. The source localized response power at the frequencies of interest were correlated with the corresponding outlier detection performance, across subjects. The areas of significant correlation are plotted here (same color scale for all plots). Sentence and equation rates are significantly correlated with behavior only if attended, while both attended and unattended word rates are significantly correlated with behavior. Sentence rate power is significantly correlated over regions in left temporal, parietal and frontal areas, while significant correlation for the equation rate power is seen in left parietal and occipital regions.

3.4. TRF analysis

TRF analysis was performed using source localized MEG time signals for each condition (details in Methods 2.7). TRFs were simultaneously obtained for responses to the acoustic envelopes, word/symbol onsets and sentence/equation onsets. The envelope and word/symbol TRFs were not

used for further analysis, since they were dominated by acoustic responses that have been well-studied in other investigations (Brodbeck et al., 2018a, 2018b). Critically, however, including such envelopes and word/symbol TRFs in the same model separates their responses from those of higher level processing, providing cleaner TRFs for sentences and equations, now well separated from responses due to auditory processing. The volume source localized TRFs are time-varying vectors at each voxel. Activity of nearby neural populations may overlap, even if the activity is driven by different processes, due to the limited spatial resolution of MEG. However, these effects may have different current directions due to the anatomy of the cortical surface. Therefore, a test for consistent vector directions, using Hotelling's T^2 statistic and permutation tests with TFCE, was used to detect group differences in the direction of current flow (see Methods 2.9).

The sentence and equation TRFs showed significance over several time intervals and many voxels over the duration of the TRF ($T^2_{max} = 7.34$, $p_{min} < 0.001$, and $T^2_{max} = 5.52$, $p_{min} < 0.001$, respectively, see Fig 5). The TRFs are computed starting from 350 ms after the sentence onset to 350 ms after the end of the sentence, but because of the fixed-period presentation rate without any breaks between sentences in a trial, the TRFs from 0-350 ms are identical to the last 350 ms. The large peak at the end (and beginning) of each TRF may either arise from processing of the completion of the sentence/equation, or to preparation (or auditory) processing of the new sentence sentence/equation, or both. This peak occurs around 60-180 ms after the start of the new sentence/equation, in the typical latency range of early auditory processing. However, spatial distributions of the peak in the equation TRFs seem to indicate patterns that are not consistent with purely auditory processing, especially for the cocktail party condition (described below). Additionally, significant activity is seen throughout the duration of the sentence/equation that is

not tied to word/symbol onsets, indicating that lower-level auditory responses have been successfully regressed out. Therefore, the large peaks at the end probably reflect processing of the completion of the sentence/equation (with a latency of 430-540 ms after the last word/symbol). The sentence TRF peaks were significant predominantly in the left temporal lobe, while the equation TRF peaks were significant in bilateral temporal, parietal and motor areas.

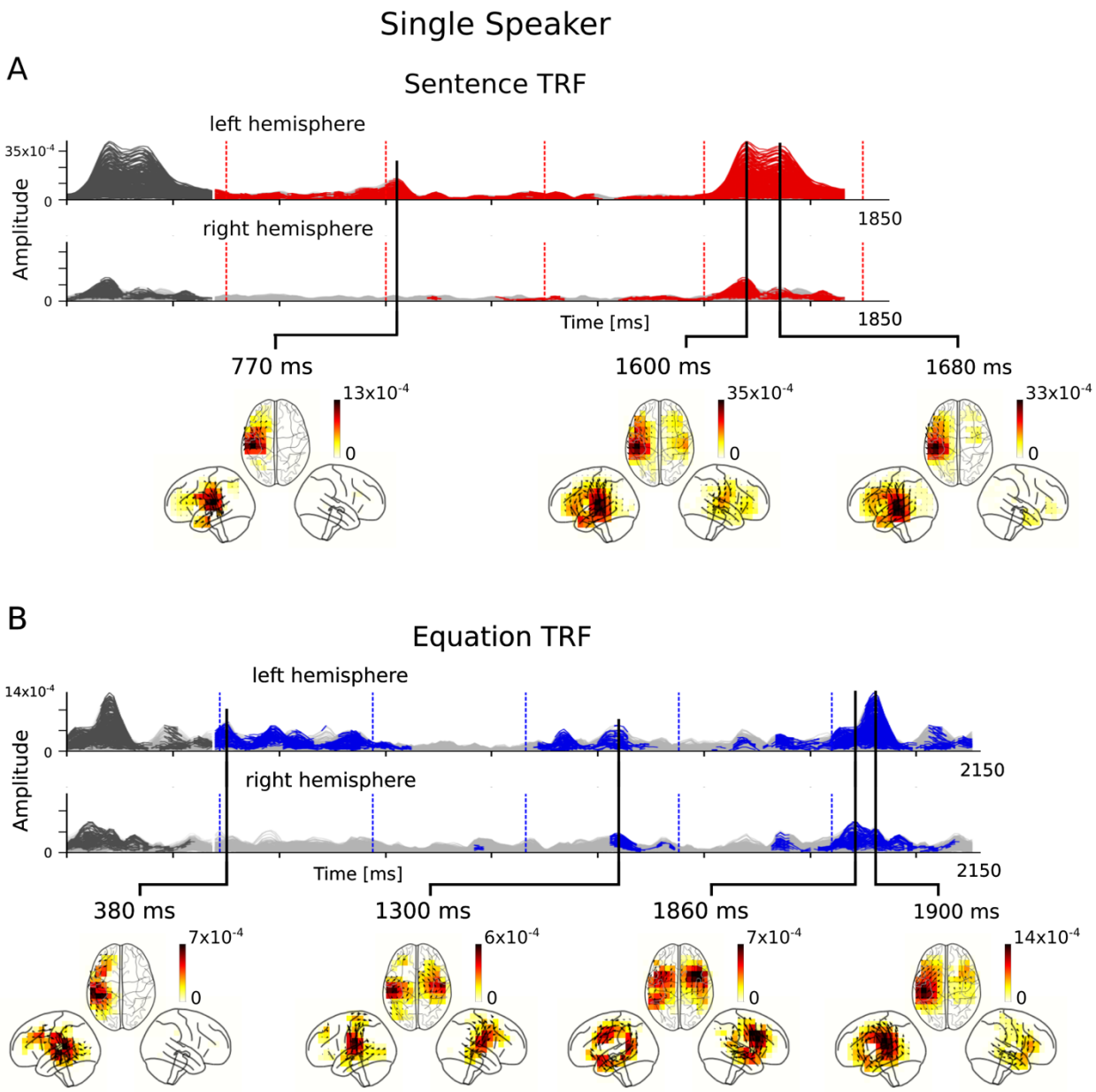

Figure 5. TRFs in the single speaker conditions. Overlay plots of the amplitude of the TRF vectors for each voxel, averaged over subjects. For each TRF subfigure, the top axis shows vector amplitudes of voxels in the left hemisphere and the bottom axis correspondingly in the right hemisphere. Each trace is from the TRF of a single voxel; non-significant time points are shown in gray, while significant time points are shown in red (sentence processing) or blue (equation processing). The duration plotted corresponds to that of sentence or equation, plus 350 ms; because of the fixed presentation rate, the first 350 ms (shown in gray) are identical to the last 350 ms. The large peak at the end (and beginning) of each TRF may either be ascribed to processing of the completion of the sentence/equation, or to the onset of the new sentence sentence/equation, or both. Word and symbol onset times are shown in red and blue dashed lines respectively; it can be seen that response contributions associated with them have been successfully regressed out. Volume source space distributions for several peaks in the TRF amplitudes are shown in the inlay plots (color scales normalized within each inlay to highlight spatial patterns), with black arrows denoting current directions (peaks automatically selected as local maxima of the TRFs). Although most of the TRF activity is dominated by neural currents in the left temporal lobe, the equation TRFs show more bilateral activation. The full time-courses of all significant neural source space distributions are shown in Video 1.

Video 1. TRFs in the single speaker conditions. The sentence and equation TRFs are shown from 350 ms until 350 ms past the end of the sentence or equation. Traces at significant time points are shown in red (sentence processing) or blue (equation processing). The distribution of cortical activity at each time point is shown on the right, with color scales fixed over each entire TRF.

Differences in sentence and equation processing were more readily visible in the TRFs for the cocktail party conditions. The test for consistent vector direction revealed similar results to the single speaker conditions (sentence TRF T^2_{max} = 5.88, p_{min} < 0.001, equation TRF T^2_{max} = 5.06, p_{min} < 0.001) as shown in Fig 6, however, the differences between sentences and equations were more pronounced, especially at for the later peaks 430-620 ms after the onset of the last word or

symbol. The peaks in the equation TRF were localized to left motor and parietal regions and right inferior frontal areas that are associated with arithmetic processing. This strengthens the hypothesis that these late peaks indicate lagged higher-level processing of the completed equation and not early auditory/preparatory processing of the subsequent equation. Although the cortical localization of sentence TRF peaks remain consistent in left temporal areas throughout most of the time course, the equation TRF peaks show several distinct cortical patterns, and may reflect distinct processes. The equation TRF was significant for several time intervals in the right hemisphere (more than in the single speaker case) and showed strong activity in IPS, superior parietal and motor areas, while sentence TRFs consistently localized predominantly to regions near left auditory cortex (even more so than in the single speaker case). Therefore, selective attention in the cocktail conditions seems to highlight differences between arithmetic and language processing, and possible explanations are discussed section 4.6.

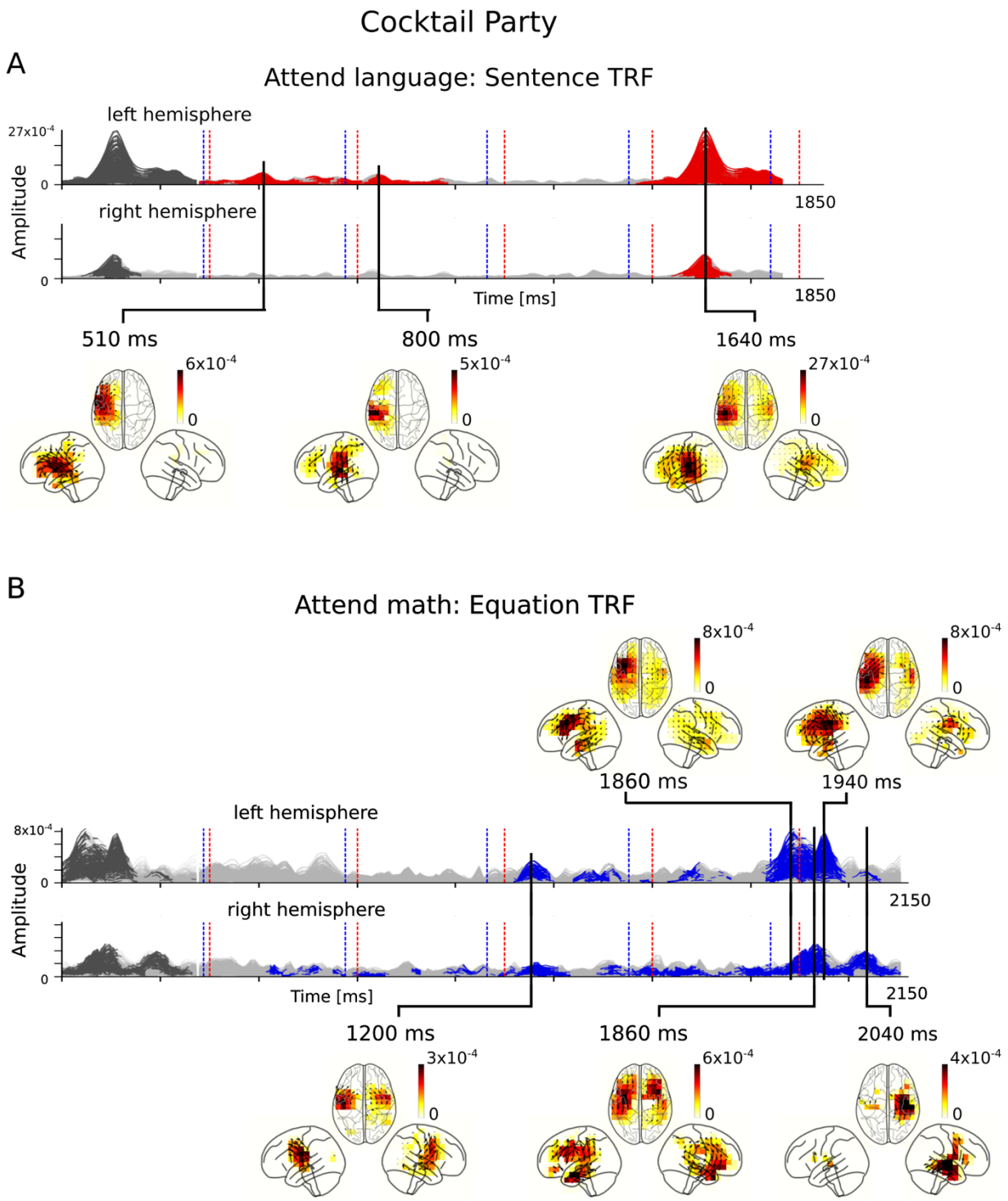

Figure 6. TRFs in the cocktail party conditions. Overlay plots of the TRF for each voxel averaged over subjects are shown similar to those in Fig. 5. Word and symbol onset times are shown in red and blue dashed lines respectively and are marked in both sentence and equation TRFs since both stimuli were present in the

cocktail party conditions; again, it can be seen that responses contributions associated with them have been successfully regressed out. Differences between sentence and equation TRFs arise at later time points, with sentence TRFs being predominantly near left temporal areas, while equation TRFs are in bilateral temporal, motor and parietal regions. The entire sentence and equation TRFs are shown in Video 2.

Video 2. TRFs in the cocktail party conditions. The sentence and equation TRFs are shown from 350 ms until 350 ms past the end of the sentence or equation. Traces at significant time points are shown in red (sentence processing) or blue (equation processing). The distribution of cortical activity at each time point is shown on the right, with color scales fixed over each entire TRF.

3.5. Decoder analysis

To further help differentiate between the cortical processing of math and language, two types of linear decoders were trained on responses. 1) Classifiers at each time point that learned weights based on the MEG sensor topography at that time point. 2) Classifiers at each voxel that learned weights based on the temporal dynamics of the response at that voxel. The former was used to contrast the dynamics of math and language processing (Fig. 7A). For the single speaker conditions, all time points showed significant decoding ability across subjects (t_{max} = 11.3, p_{min} < 0.001), with higher prediction success (as measured by *AUC*) at longer latencies. For the cocktail party conditions, decoding ability was significantly above chance only at longer latencies (t_{max} = 6.45, p_{min} < 0.001). While subjects listened to the equations, the identity of the arithmetic operator (e.g., 'plus' vs. 'times' or 'less') was reliably decoded from the MEG sensor topography during the time points when the operator and the subsequent operand were presented (Fig. 7B).

Decoders at each voxel were also trained to differentiate attention to arithmetic vs. language, based on the dynamics of the response at that voxel during the first or last words (Fig. 7C). The prediction success (as measured by *AUC*) was significant for large areas in the single speaker conditions both for first words ($t_{max} = 5.1$, $p_{min} < 0.001$) and last words ($t_{max} = 5.4$, $p_{min} < 0.001$) decoders. The *AUC* for first words decoders was significant for all regions in the left hemisphere except for areas in the inferior and middle temporal gyrus and all regions on the right hemisphere except the occipital lobe. The *AUC* for last words was significant for all regions in the left hemisphere and parts of frontal temporal lobes in the right hemisphere. For the cocktail party conditions the source-localized regions of significant prediction success were much more focal: the *AUC* was significant only in the IPS and superior parietal areas for both first words ($t_{max} = 5.3$, $p_{min} < 0.001$) and last words ($t_{max} = 4.3$, $p_{min} = 0.014$) decoders. These results suggest that the activity of voxels in left IPS and superior parietal areas most useful for discriminating between attending to arithmetic vs. language. Finally, decoders at each voxel were also trained to decode the attention condition (foreground vs. background) from the response to the entire sentence or equation (Fig 7D). The *AUC* was significant in bilateral parietal areas for decoding whether arithmetic was in foreground vs. background ($t_{max} = 5.2$, $p_{min} < 0.001$), consistent with areas involved in arithmetic processing. For decoding whether language was in foreground vs. background, the *AUC* was significant ($t_{max} = 5.1$, $p_{min} = 0.002$) in left middle temporal areas (consistent with higher level language processing) and bilateral superior parietal areas (consistent with attention networks that are involved in discriminating auditory stimuli). Therefore, the decoding analysis is able to detect different cortical areas that may be involved in attention to language and arithmetic.

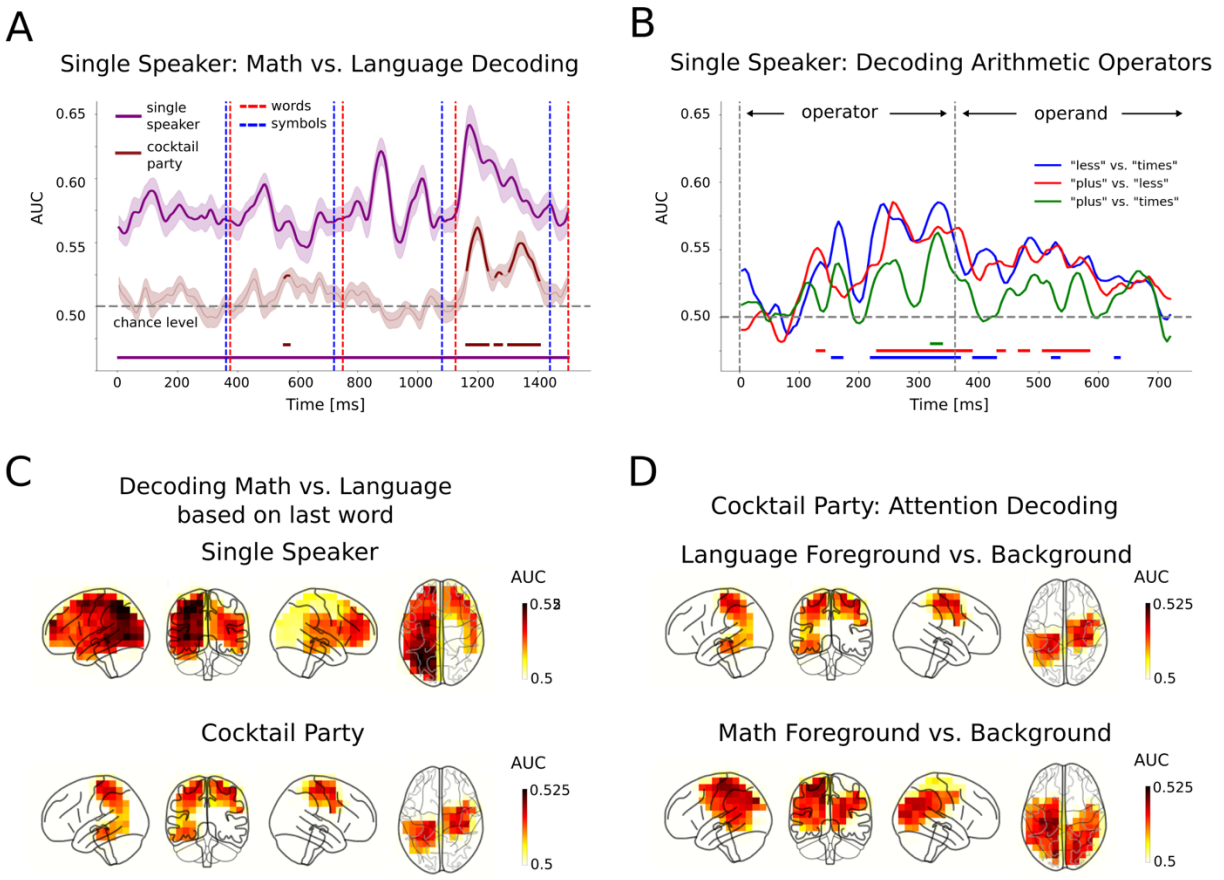

Figure 7. Decoding arithmetic and language processing. A. Performance of decoding attention condition (math vs. language) at each time point using MEG sensors for single speaker and cocktail party. Prediction success is measured by *AUC*, which is plotted (mean and s.e.m. across subjects); time points where predictions are significantly above chance are marked by the horizontal purple bar at the bottom (every time point is significantly above chance). The word and symbol onsets are also shown, and the decoding performance increases towards the end of the time window. **B.** Decoding arithmetic operators from sensor topographies. The time window of the operator and the subsequent operand was used for the 3 types of decoders. Time intervals where predictions are significantly above chance are marked by the colored horizontal bars at the bottom: all 3 operator comparisons could be significantly decoded. **C.** Decoding math vs. language based on the last word. During the single speaker conditions, most of the brain is significant. However, for the cocktail party conditions, more focal significant decoding is seen in IPS and superior parietal areas. Decoding based on the first word resulted in similar results (not shown). **D.** Decoding attention in the cocktail party conditions (*AUC* masked by

significance across subjects). The sentence responses in foreground and background were decoded in left middle temporal and bilateral superior parietal areas. The equation responses in foreground and background were decoded in bilateral parietal areas.

4 Discussion

4.1. Cortical tracking of equations and sentences

As expected, MEG responses to acoustic features source-localize to bilateral auditory cortex, and neural tracking of sentences source-localizes to left temporal cortex, consistent with areas known for sentence and speech processing (Friederici, 2002, 2011; Vandenberghe et al., 2002; Hickok and Poeppel, 2007; Binder et al., 2009), similar to prior isochronous speech studies (Sheng et al., 2018). In contrast, we find neural equation tracking localizes to left parietal, temporal and occipital areas. Arithmetic processing can activate IPS and parietal areas (Dehaene et al., 2003), angular gyrus (Göbel et al., 2001), temporal regions (Tang et al., 2006), and occipital areas (Maruyama et al., 2012; Harvey and Dumoulin, 2017), perhaps due to internal visualization (Zago et al., 2001). Equation tracking also localizes to right temporal and parietal areas in the cocktail party conditions, confirming that arithmetic processing is more bilateral than language processing (Dehaene and Cohen, 1997; Amalric and Dehaene, 2018, 2019). Unexpectedly, significant neural tracking of the ignored sentence and equation rates was found in smaller temporal and parietal areas respectively. Subjects may have been unable to wholly sustain attention to the foreground for the entirety of this diotic stimulus and may have briefly switched the focus of attention. These regions too are consistent with language and arithmetic processing for each case, providing further evidence that these responses are not merely tracking sentential structure, but rather the content.

4.2. Left hemispheric dominance of equation tracking

The responses to equations were significantly left lateralized in the single speaker conditions and left dominant in the cocktail party conditions. This could reflect left lateralized language processing, since equations were presented using speech. However, arithmetic processing may also show left dominance (Pinel and Dehaene, 2009), perhaps due to precise calculations (Dehaene, 1999; Pica et al., 2004) or arithmetic fact retrieval (Dehaene et al., 2003; Grabner et al., 2009). These fast-paced stimuli required rapid calculations, and may have resulted in increased left hemispheric activity due to increased reliance on rote memory (Campbell and Austin, 2002). Specific strategies employed for calculation may also result in left lateralized responses—multiplication of small numbers is often performed using rote memory which activates left hemispheric areas (Delazer et al., 1999; Ischebeck et al., 2006; Fehr et al., 2007), while subtraction is less commonly performed using memory and shows more bilateral activation (Schmithorst and Brown, 2004; Prado et al., 2011). Addition may recruit both these networks, depending on specific strategies utilized by individuals (Arsalidou and Taylor, 2011). We found no significant differences in equation responses when separated by operation type, perhaps because of individual variation in procedural calculation or retrieval strategies within the same operation (Tschentscher and Hauk, 2014). However, operation types were successfully decoded from the overall MEG signals (Fig. 8B), consistent with prior work (Pinheiro-Chagas et al., 2019), though this effect was not as robust as decoding stimulus type or attention. Overall, left hemispheric dominance of equation tracking is supported by a combination of speech processing, precise calculations, and arithmetic fact retrieval.

4.3. Cortical correlates of behavioral performance

Neural tracking of sentence, equation, word and symbol rates was correlated with performance in detecting deviants, consistent with language-only isochronous studies (Ding et al., 2017). Sentence tracking correlated with accuracy of sentence deviant detection in language areas, such as left auditory cortex, superior and middle temporal lobe and angular gyrus (Price, 2000; Binder et al., 2009; Karuza et al., 2013) in both the single speaker and the cocktail party conditions. In contrast, performance in detecting deviant equations in the cocktail party conditions correlated with equation tracking in posterior parietal areas, which are known to predict competence and performance in numerical tasks (Grabner et al., 2007; Lin et al., 2012, 2019; Lasne et al., 2019). The lack of significant behavioral correlations for equation tracking in the single speaker conditions may be due to several subjects performing at ceiling; equations had a restricted set of only 14 unique symbols, and the presence of the 'is' symbol in every equation might be structurally useful in tracking equation boundaries. Unexpectedly, significant correlation with behavior was seen for background symbol rate responses in parietal and occipital areas (and for background word rate responses in a small parietal region). Some studies show that acoustic features of background speech may also be tracked (Fiedler et al., 2019; Brodbeck et al., 2020). Since the background word and symbol rates are present in the stimulus acoustics, increased effort or attention could enhance both behavioral performance and auditory responses at these rates. Representations of the background could enhance attentional selectivity in challenging cocktail party environments as suggested by Fiedler et al., 2019. However, note that sentence and equation tracking was only correlated with behavior when in the foreground. Overall, these results suggest cortical tracking may reflect improved comprehension due to neural chunking of speech structures (Blanco-Elorrieta et al., 2019; Chen et al., 2020; Jin et al., 2020; Kaufeld et al., 2020; Teng et al.,

2020). Behavioral correlations with equation tracking in parietal and occipital areas further indicate they may be linked to successful calculations.

4.4. Dynamics of arithmetic and language processing

Responses to higher level speech features have been previously segregated from those due to purely auditory processing, by jointly estimating TRFs to linguistic and acoustic features (Brodbeck et al., 2018a, 2018b; Broderick et al., 2018). Analogously, we jointly estimated TRFs to equation and sentence onsets along with the speech envelope. We find equation TRFs differ from sentence TRFs, especially so at longer latencies. Prior studies have found late evoked responses specific to numbers and equations (Avancini et al., 2015). However, unlike evoked responses, our TRFs investigate arithmetic processing during continuous speech and selective attention, while regressing out responses due to acoustics and individual symbols. Large peaks appear in both sentence and equation TRFs 430–620 ms after the onset of the last word/symbol and may reflect processing of the completion of the sentence/equation. Sentence TRF peaks localize to left temporal areas, while equation TRF peaks show distinct activity patterns in bilateral parietal and temporal areas involved in numerical processing (Abd Hamid et al., 2011; Amalric and Dehaene, 2018), and motor areas, perhaps reflecting procedural calculation strategies (Tschentscher and Hauk, 2014). The latencies and locations of these peaks are similar to prior arithmetic ERP studies (Iguchi and Hashimoto, 2000; Iijima and Nishitani, 2017). The cortical patterns of TRF peaks show more differences in the cocktail party than the single speaker conditions, suggesting that selective attention focuses the underlying cortical networks.

4.5 Decoding the processing of equations and sentences

Numbers and arithmetic operations have been previously decoded from cortical responses (Eger et al., 2009; Pinheiro-Chagas et al., 2019). In this study, the attended stimulus type (math or language) was reliably decoded from MEG signals. In the single speaker conditions, decoding accuracy was significantly above chance in large regions of cortex, perhaps due to highly correlated responses across cortex for this task. In contrast, decoding accuracy during the cocktail party conditions was significant in left IPS and superior parietal areas suggesting that these regions are most important for discriminating between arithmetic and language processing. Decoding the attend-arithmetic state was significant in bilateral parietal areas, consistent with arithmetic processing. However, decoding the attend-language state was significant in left middle temporal lobe, consistent with language processing (Hickok and Poeppel, 2007). Additionally, both the attend-arithmetic and the attend-language states could be decoded from bilateral superior parietal areas. This could be due to general attentional networks in fronto-parietal areas, or attentional segregation of foreground and background speech based on pitch or gender (Hill and Miller, 2010; Kristensen et al., 2013). Overall, MEG responses contain enough information to decode arithmetic vs. language processing, selective attention and arithmetic operations.

4.6 The cocktail party paradigm highlights distinct cortical processes

Differences in source-localized sentence and equation responses were more prominent in the cocktail party than in the single speaker conditions for all analyses (frequency tracking, TRFs and decoders). Responses to both stimuli played simultaneously may have helped control for common auditory and pre-attentive responses. Abd Hamid et al., (2011) found fMRI activation in broader areas for spoken arithmetic with a noisy background than in quiet, perhaps due to increased effort.

However, in our case, the background stimulus was not white noise, but rather meaningful non-mathematical speech. Our TRF analysis, which regresses out activity due to background speech, as well as the selective attention task itself, may highlight specific cortical processes that best separate the arithmetic and language stimuli.

In summary, we show that neural tracking of spoken equations and sentences involves both overlapping and non-overlapping cortical networks. These responses are correlated with behavior, suggesting that increased neural tracking reflects improved comprehension and/or correct arithmetic calculations. Selective attention for equations focuses activity in temporal, parietal occipital and motor areas, and for sentences in temporal and superior parietal areas. This cocktail party paradigm is well suited to highlight the cortical networks underlying the processing of spoken arithmetic and language.

References

Abd Hamid AI, Yusoff AN, Mukari SZ-MS, Mohamad M (2011) Brain Activation during Addition and Subtraction Tasks In-Noise and In-Quiet. Malays J Med Sci MJMS 18:3–15.

Amalric M, Dehaene S (2016) Origins of the brain networks for advanced mathematics in expert mathematicians. Proc Natl Acad Sci 113:4909–4917.

Amalric M, Dehaene S (2018) Cortical circuits for mathematical knowledge: evidence for a major subdivision within the brain's semantic networks. Philos Trans R Soc B Biol Sci 373:20160515.

Amalric M, Dehaene S (2019) A distinct cortical network for mathematical knowledge in the human brain. NeuroImage 189:19–31.

Arsalidou M, Taylor MJ (2011) Is 2+2=4? Meta-analyses of brain areas needed for numbers and calculations. NeuroImage 54:2382–2393.

Avancini C, Soltész F, Szűcs D (2015) Separating stages of arithmetic verification: An ERP study with a novel paradigm. Neuropsychologia 75:322–329.

Baggio G, Hagoort P (2011) The balance between memory and unification in semantics: A dynamic account of the N400. Lang Cogn Process 26:1338–1367.

Baldo JV, Dronkers NF (2007) Neural correlates of arithmetic and language comprehension: A common substrate? Neuropsychologia 45:229–235.

Bemis DK, Pylkkänen L (2013) Basic linguistic composition recruits the left anterior temporal lobe and left angular gyrus during both listening and reading. Cereb Cortex N Y N 1991 23:1859–1873.

Binder JR, Desai RH, Graves WW, Conant LL (2009) Where Is the Semantic System? A Critical Review and Meta-Analysis of 120 Functional Neuroimaging Studies. Cereb Cortex 19:2767–2796.

Blanco-Elorrieta E, Ding N, Pylkkänen L, Poeppel D (2020) Understanding Requires Tracking: Noise and Knowledge Interact in Bilingual Comprehension. J Cogn Neurosci 32:1975–1983.

Boersma P, Weenick D (2018) Praat: doing phonetics by computer [Computer program]. Version 6.0.43. Available at: http://www.praat.org [Accessed September 8, 2018].

Brodbeck C, Hong LE, Simon JZ (2018a) Rapid Transformation from Auditory to Linguistic Representations of Continuous Speech. Curr Biol 28:3976-3983.e5.

Brodbeck C, Jiao A, Hong LE, Simon JZ (2020) Neural speech restoration at the cocktail party: Auditory cortex recovers masked speech of both attended and ignored speakers. PLOS Biol 18:e3000883.

Brodbeck C, Presacco A, Simon JZ (2018b) Neural source dynamics of brain responses to continuous stimuli: Speech processing from acoustics to comprehension. NeuroImage 172:162–174.

Broderick MP, Anderson AJ, Di Liberto GM, Crosse MJ, Lalor EC (2018) Electrophysiological Correlates of Semantic Dissimilarity Reflect the Comprehension of Natural, Narrative Speech. Curr Biol 28:803-809.e3.

Campbell JID, Austin S (2002) Effects of response time deadlines on adults' strategy choices for simple addition. Mem Cognit 30:988–994.

Castaldi E, Piazza M, Dehaene S, Vignaud A, Eger E (2019) Attentional amplification of neural codes for number independent of other quantities along the dorsal visual stream Gold JI, Ansari D, Ansari D, Harvey B, eds. eLife 8:e45160.

Chen Y, Jin P, Ding N (2020) The influence of linguistic information on cortical tracking of words. Neuropsychologia:107640.

Christian Brodbeck, Teon L Brooks, Proloy Das, Samir Reddigari, Joshua P Kulasingham (2020) christianbrodbeck/Eelbrain: 0.33. Zenodo. Available at: https://zenodo.org/record/4060224 [Accessed October 9, 2020].

Dastjerdi M, Ozker M, Foster BL, Rangarajan V, Parvizi J (2013) Numerical processing in the human parietal cortex during experimental and natural conditions. Nat Commun 4:2528.

David SV, Mesgarani N, Shamma SA (2007) Estimating sparse spectro-temporal receptive fields with natural stimuli. Netw Bristol Engl 18:191–212.

de Cheveigné A, Simon JZ (2007) Denoising based on Time-Shift PCA. J Neurosci Methods 165:297–305.

de Cheveigné A, Simon JZ (2008) Sensor noise suppression. J Neurosci Methods 168:195–202.

Dehaene S (1999) Sources of Mathematical Thinking: Behavioral and Brain-Imaging Evidence. Science 284:970–974.

Dehaene S, Cohen L (1997) Cerebral Pathways for Calculation: Double Dissociation between Rote Verbal and Quantitative Knowledge of Arithmetic. Cortex 33:219–250.

Dehaene S, Molko N, Cohen L, Wilson AJ (2004) Arithmetic and the brain. Curr Opin Neurobiol 14:218–224.

Dehaene S, Piazza M, Pinel P, Cohen L (2003) Three parietal circuits for number processing. Cogn Neuropsychol 20:487–506.

Delazer M, Girelli L, Semenza C, Denes G (1999) Numerical skills and aphasia. J Int Neuropsychol Soc 5:213–221.

Di Liberto GM, O'Sullivan JA, Lalor EC (2015) Low-Frequency Cortical Entrainment to Speech Reflects Phoneme-Level Processing. Curr Biol 25:2457–2465.

Ding N, Melloni L, Yang A, Wang Y, Zhang W, Poeppel D (2017) Characterizing Neural Entrainment to Hierarchical Linguistic Units using Electroencephalography (EEG). Front Hum Neurosci 11.

Ding N, Melloni L, Zhang H, Tian X, Poeppel D (2016) Cortical tracking of hierarchical linguistic structures in connected speech. Nat Neurosci 19:158–164.

Ding N, Pan X, Luo C, Su N, Zhang W, Zhang J (2018) Attention Is Required for Knowledge-Based Sequential Grouping: Insights from the Integration of Syllables into Words. J Neurosci 38:1178–1188.

Ding N, Simon JZ (2012) Emergence of neural encoding of auditory objects while listening to competing speakers. Proc Natl Acad Sci 109:11854–11859.

Eger E, Michel V, Thirion B, Amadon A, Dehaene S, Kleinschmidt A (2009) Deciphering Cortical Number Coding from Human Brain Activity Patterns. Curr Biol 19:1608–1615.

Eger E, Sterzer P, Russ MO, Giraud A-L, Kleinschmidt A (2003) A supramodal number representation in human intraparietal cortex. Neuron 37:719–725.

Fehr T, Code C, Herrmann M (2007) Common brain regions underlying different arithmetic operations as revealed by conjunct fMRI–BOLD activation. Brain Res 1172:93–102.

Fiedler L, Wöstmann M, Herbst SK, Obleser J (2019) Late cortical tracking of ignored speech facilitates neural selectivity in acoustically challenging conditions. NeuroImage 186:33–42.

Fischl B (2012) FreeSurfer. NeuroImage 62:774–781.

Friederici AD (2002) Towards a neural basis of auditory sentence processing. Trends Cogn Sci 6:78–84.

Friederici AD (2011) The Brain Basis of Language Processing: From Structure to Function. Physiol Rev 91:1357–1392.

Gelman R, Butterworth B (2005) Number and language: how are they related? Trends Cogn Sci 9:6–10.

Göbel S, Walsh V, Rushworth MFS (2001) The Mental Number Line and the Human Angular Gyrus. NeuroImage 14:1278–1289.

Grabner RH, Ansari D, Koschutnig K, Reishofer G, Ebner F, Neuper C (2009) To retrieve or to calculate? Left angular gyrus mediates the retrieval of arithmetic facts during problem solving. Neuropsychologia 47:604–608.

Grabner RH, Ansari D, Reishofer G, Stern E, Ebner F, Neuper C (2007) Individual differences in mathematical competence predict parietal brain activation during mental calculation. NeuroImage 38:346–356.

Gramfort A (2013) MEG and EEG data analysis with MNE-Python. Front Neurosci 7.

Gramfort A, Luessi M, Larson E, Engemann DA, Strohmeier D, Brodbeck C, Parkkonen L, Hämäläinen MS (2014) MNE software for processing MEG and EEG data. NeuroImage 86:446–460.

Hämäläinen MS, Ilmoniemi RJ (1994) Interpreting magnetic fields of the brain: minimum norm estimates. Med Biol Eng Comput 32:35–42.

Harvey BM, Dumoulin SO (2017) A network of topographic numerosity maps in human association cortex. Nat Hum Behav 1:1–9.

Harvey BM, Klein BP, Petridou N, Dumoulin SO (2013) Topographic Representation of Numerosity in the Human Parietal Cortex. Science 341:1123–1126.

Hickok G, Poeppel D (2007) The cortical organization of speech processing. Nat Rev Neurosci 8:393–402.

Hill KT, Miller LM (2010) Auditory Attentional Control and Selection during Cocktail Party Listening. Cereb Cortex 20:583–590.

Houdé O, Tzourio-Mazoyer N (2003) Neural foundations of logical and mathematical cognition. Nat Rev Neurosci 4:507–514.

Iguchi Y, Hashimoto I (2000) Sequential information processing during a mental arithmetic is reflected in the time course of event-related brain potentials. Clin Neurophysiol 111:204–213.

Iijima M, Nishitani N (2017) Cortical dynamics during simple calculation processes: A magnetoencephalography study. Clin Neurophysiol Pract 2:54–61.

Ischebeck A, Zamarian L, Siedentopf C, Koppelstätter F, Benke T, Felber S, Delazer M (2006) How specifically do we learn? Imaging the learning of multiplication and subtraction. NeuroImage 30:1365–1375.

Jasinski EC, Coch D (2012) ERPs across arithmetic operations in a delayed answer verification task. Psychophysiology 49:943–958.

Jin P, Lu Y, Ding N (2020) Low-frequency neural activity reflects rule-based chunking during speech listening Reichenbach T, Shinn-Cunningham BG, Reichenbach T, eds. eLife 9:e55613.

Karuza EA, Newport EL, Aslin RN, Starling SJ, Tivarus ME, Bavelier D (2013) The neural correlates of statistical learning in a word segmentation task: An fMRI study. Brain Lang 127:46–54.

Kaufeld G, Bosker HR, Oever S ten, Alday PM, Meyer AS, Martin AE (2020) Linguistic Structure and Meaning Organize Neural Oscillations into a Content-Specific Hierarchy. J Neurosci 40:9467–9475.

Koelsch S, Kasper E, Sammler D, Schulze K, Gunter T, Friederici AD (2004) Music, language and meaning: brain signatures of semantic processing. Nat Neurosci 7:302–307.

Kou H, Iwaki S (2007) Modulation of neural activities by the complexity of mental arithmetic: An MEG study. Int Congr Ser 1300:539–542.

Kristensen LB, Wang L, Petersson KM, Hagoort P (2013) The Interface Between Language and Attention: Prosodic Focus Marking Recruits a General Attention Network in Spoken Language Comprehension. Cereb Cortex 23:1836–1848.

Ku Y, Hong B, Gao X, Gao S (2010) Spectra-temporal patterns underlying mental addition: An ERP and ERD/ERS study. Neurosci Lett 472:5–10.

Lalor EC, Foxe JJ (2010) Neural responses to uninterrupted natural speech can be extracted with precise temporal resolution. Eur J Neurosci 31:189–193.

Lasne G, Piazza M, Dehaene S, Kleinschmidt A, Eger E (2019) Discriminability of numerosity-evoked fMRI activity patterns in human intra-parietal cortex reflects behavioral numerical acuity. Cortex 114:90–101.

Lau EF, Phillips C, Poeppel D (2008) A cortical network for semantics: (de)constructing the N400. Nat Rev Neurosci 9:920–933.

Lin J-FL, Imada T, Kuhl PK (2012) Mental Addition in Bilinguals: An fMRI Study of Task-Related and Performance-Related Activation. Cereb Cortex 22:1851–1861.

Lin J-FL, Imada T, Kuhl PK (2019) Neuroplasticity, bilingualism, and mental mathematics: A behavior-MEG study. Brain Cogn 134:122–134.

Luo C, Ding N (2020) Cortical encoding of acoustic and linguistic rhythms in spoken narratives. eLife 9

Mardia KV (1975) Assessment of Multinormality and the Robustness of Hotelling's T2 Test. J R Stat Soc Ser C Appl Stat 24:163–171.

Maruyama M, Pallier C, Jobert A, Sigman M, Dehaene S (2012) The cortical representation of simple mathematical expressions. NeuroImage 61:1444–1460.

Menon V, Rivera SM, White CD, Glover GH, Reiss AL (2000) Dissociating Prefrontal and Parietal Cortex Activation during Arithmetic Processing. NeuroImage 12:357–365.

Monti MM, Parsons LM, Osherson DN (2012) Thought Beyond Language: Neural Dissociation of Algebra and Natural Language. Psychol Sci.

Nichols TE, Holmes AP (2002) Nonparametric permutation tests for functional neuroimaging: A primer with examples. Hum Brain Mapp 15:1–25.

Obleser J, Lahiri A, Eulitz C (2003) Auditory-evoked magnetic field codes place of articulation in timing and topography around 100 milliseconds post syllable onset. NeuroImage 20:1839–1847.

Obleser J, Lahiri A, Eulitz C (2004) Magnetic Brain Response Mirrors Extraction of Phonological Features from Spoken Vowels. J Cogn Neurosci 16:31–39.

Park J, Hebrank A, Polk TA, Park DC (2011) Neural Dissociation of Number from Letter Recognition and Its Relationship to Parietal Numerical Processing. J Cogn Neurosci 24:39–50.

Pedregosa F, Varoquaux G, Gramfort A, Michel V, Thirion B, Grisel O, Blondel M, Prettenhofer P, Weiss R, Dubourg V, Vanderplas J, Passos A, Cournapeau D (2011) Scikit-learn: Machine Learning in Python. J Mach Learn Res:6.

Pica P, Lemer C, Izard V, Dehaene S (2004) Exact and Approximate Arithmetic in an Amazonian Indigene Group. Science 306:499–503.

Pinel P, Dehaene S (2009) Beyond Hemispheric Dominance: Brain Regions Underlying the Joint Lateralization of Language and Arithmetic to the Left Hemisphere. J Cogn Neurosci 22:48–66.

Pinel P, Dehaene S, Rivière D, LeBihan D (2001) Modulation of Parietal Activation by Semantic Distance in a Number Comparison Task. NeuroImage 14:1013–1026.

Pinheiro-Chagas P, Piazza M, Dehaene S (2019) Decoding the processing stages of mental arithmetic with magnetoencephalography. Cortex 114:124–139.

Prado J, Mutreja R, Zhang H, Mehta R, Desroches AS, Minas JE, Booth JR (2011) Distinct representations of subtraction and multiplication in the neural systems for numerosity and language. Hum Brain Mapp 32:1932–1947.

Price CJ (2000) The anatomy of language: contributions from functional neuroimaging. J Anat 197:335–359.

Schmithorst VJ, Brown RD (2004) Empirical validation of the triple-code model of numerical processing for complex math operations using functional MRI and group Independent Component Analysis of the mental addition and subtraction of fractions. NeuroImage 22:1414–1420.

Sheng J, Zheng L, Lyu B, Cen Z, Qin L, Tan LH, Huang M-X, Ding N, Gao J-H (2018) The Cortical Maps of Hierarchical Linguistic Structures during Speech Perception. Cereb Cortex.

Smith SM, Nichols TE (2009) Threshold-free cluster enhancement: Addressing problems of smoothing, threshold dependence and localisation in cluster inference. NeuroImage 44:83–98.

Spelke ES, Tsivkin S (2001) Language and number: a bilingual training study. Cognition 78:45–88.

Tang Y, Zhang W, Chen K, Feng S, Ji Y, Shen J, Reiman EM, Liu Y (2006) Arithmetic processing in the brain shaped by cultures. Proc Natl Acad Sci 103:10775–10780.

Teng X, Ma M, Yang J, Blohm S, Cai Q, Tian X (2020) Constrained Structure of Ancient Chinese Poetry Facilitates Speech Content Grouping. Curr Biol 30:1299-1305.e7.

Tschentscher N, Hauk O (2014) How are things adding up? Neural differences between arithmetic operations are due to general problem solving strategies. NeuroImage 92:369–380.

Vandenberghe R, Nobre AC, Price CJ (2002) The Response of Left Temporal Cortex to Sentences. J Cogn Neurosci 14:550–560.

Varley RA, Klessinger NJC, Romanowski CAJ, Siegal M (2005) Agrammatic but numerate. Proc Natl Acad Sci U S A 102:3519–3524.

Venkatraman V, Siong SC, Chee MWL, Ansari D (2006) Effect of Language Switching on Arithmetic: A Bilingual fMRI Study. J Cogn Neurosci 18:64–74.

Zago L, Pesenti M, Mellet E, Crivello F, Mazoyer B, Tzourio-Mazoyer N (2001) Neural Correlates of Simple and Complex Mental Calculation. NeuroImage 13:314–327.

Zarnhofer S, Braunstein V, Ebner F, Koschutnig K, Neuper C, Reishofer G, Ischebeck A (2012) The Influence of verbalization on the pattern of cortical activation during mental arithmetic. Behav Brain Funct 8:13.